Journal of Inorganic and General Chemistry
ZAAC
Zeitschrift für anorganische und allgemeine Chemie
www.zaac.wiley-vch.de
RESEARCH ARTICLE

DOI: 10.1002/zaac.202200085

A Versatile Route To Cyclic (Alkyl)(Amino)Carbene-Stabilized Stibinidenes

Michael S. M. Philipp[a] and Udo Radius*[a]

Dedicated to Professor Dr. Dieter Fenske on the occasion of his 80th birthday.

A convenient route for the synthesis of the cAAC^{Me} (cAAC = cyclic (alkyl)(amino)carbene, cAAC^{Me} = 1-(2,6-di-*iso*-propylphenyl)-3,3,5,5-tetramethyl-pyrrolidin-2-ylidene) and cAAC^{Cy} (cAAC^{Cy} = 2-azaspiro[4.5]dec-2-(2,6-diisopropylphenyl)-3,3-dimethyl-1-ylidene) stabilized stibinidenes cAAC^{Me}·SbMes (**2a**) (Mes = 2,4,6-trimethylphenyl) and cAAC^{Cy}·SbMes (**2b**) is reported. A mechanism for the formation of [cAAC^{R}Cl][$SbCl_3$Mes] **1** and cAAC^{R}·SbMes **2** from the reaction of cAAC with the antimony(III) precursor $SbCl_2$Mes, which proceeds *via* the isolable intermediate [cAAC^{R}SbClMes][$SbCl_3$Mes] (**3**), is proposed.

The application of *N*-heterocyclic carbenes (NHCs)[1] and related molecules such as cyclic (alkyl)(amino)carbenes (cAACs)[2] in main group chemistry has led to impressive improvements in this field over the last decade. For example, significant progress has been achieved in the stabilization and isolation of *Lewis* acid/base adducts with highly tunable NHC ligands in their stereo-electronic properties, in the chemistry of low-coordinate main group element compounds and in the substrate activation using low-valent main group element compounds.[3]

For group 15 elements, NHCs and related molecules have been applied especially in phosphorous chemistry for the synthesis of NHC-phosphenium salts and the synthesis of phosphino and phosphonio-substituted carbenes, for the preparation of carbene-stabilized main group diatomic and polyatomic allotropes and in the generation of carbene-stabilized phosphinides and in phosphinide transfer reactions using NHC-phosphinidenes.[4] Typical synthetic pathways to NHC-phosphinidenes (NHC·PR) are the reduction of adducts NHC·PCl_2R,[5] the cleavage of *cyclo*-phosphines 1/n$(RP)_n$ with carbenes,[6] the dehydrogenative coupling of RPH_2 in the presence of NHCs,[7] and the use of different other phosphinidene precursors.[8] This research also led to the development of related carbene-stabilized arsinidenes[6a,5] as well as other arsenic compounds.[1,6]

Compared to the lighter group 15 homologues, the chemistry of low-valent NHC-stabilized antimony compounds is still in its infancy. However, it has been demonstrated previously that NHC- and cAAC-stabilized antimony(III) precursors are valuable starting materials for the development of antimony main group chemistry. The synthesis of the Sb(II) radical (cAAC^{Cy})·$SbCl_2^{\bullet}$ (cAAC^{Cy} = 2-azaspiro[4.5]dec-2-(2,6-diisopropylphenyl)-3,3-dimethyl-1-ylidene) (Scheme 1, **C**) was realized by reduction of (cAAC^{Cy})·$SbCl_3$ using one equivalent of KC_8. The reduction with two equivalents of KC_8 led to formation of the cAAC-stabilized stibinidene (cAAC^{Cy})·SbCl (Scheme 1, **B**) and reduction with three equivalents to the stiba-alkene dimer [(cAAC^{Cy})Sb]$_2$ (Scheme 1, **F**), respectively.[11] The first aryl-substituted carbene-stabilized stibinidene (DAC^{Mes})·SbPh (DAC^{Mes} = 1,3-dimesityl-5,5-dimethyl-4,6-dioxo-3,4,5,6-tetrahydro-pyrimidine-2-ylidene; Scheme 1, **A**) was prepared *via* reduction of (DAC^{Mes})·$SbCl_2$Ph.[12] Furthermore, it was reported previously that the reduction of SbX_3 (X = F, Cl) with KC_8 in the presence of cAAC^{Me} (cAAC^{Me} = 1-(2,6-di-*iso*-propylphenyl)-3,3,5,5-tetrameth-

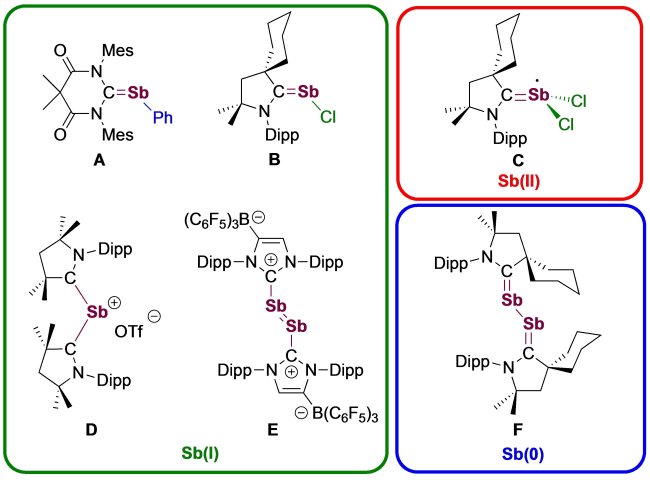

Scheme 1. Carbene stabilized Sb(II), Sb(I) and Sb(0) compounds.

[a] *M. S. M. Philipp, Prof. Dr. U. Radius*
Institute of Inorganic Chemistry, Julius-Maximilians-Universität Würzburg
Am Hubland, 97074 Würzburg, Germany
E-mail: u.radius@uni-wuerzburg.de
Homepage: http://www.ak-radius.de

Supporting information for this article is available on the WWW under https://doi.org/10.1002/zaac.202200085

yl-pyrrolidin-2-ylidene) and LiOTf (LiOTf = $LiCF_3SO_3$) in a molar ratio of 1:2:2:2 afforded $[(cAAC^{Me})_2Sb][OTf]$ (Scheme 1, **D**) featuring an anionic, cAAC-stabilized antimony(I) center.[13] The NHC-stabilized distibene $[^a(B(C_5F_5)_3)\text{-}Dipp_2Im)\cdot Sb]_2$ ($Dipp_2Im$ = 1,3-di-(2,6-di-*iso*propylphenyl)-imidazolin-2-ylidene) (Scheme 1, **E**) was synthesized *via* metallic reduction of $^a(B(C_5F_5)_3)\text{-}Dipp_2Im)\cdot SbCl_2$.[14]

We recently reported the synthesis and characterization of a number of carbene-stabilized antimony(III) compounds.[15] In course of these studies on *Lewis* acid/base adducts of NHCs and cAACs with the chlorostibanes $SbCl_3$ and $SbCl_2R$ (R = Ph and Mes) we observed that some adducts of sterical demanding carbenes with $SbCl_2Mes$ are quite unstable, most probably due to steric repulsion.[15] For the adduct $Mes_2Im\cdot SbCl_2Mes$ (Scheme 2, **G**; R_2Im = 1,3-di-organyl-imidazolin-2-ylidene; Mes = 2,4,6-trimethylphenyl) we observed a structural change in the solid state geometry compared to adducts of sterically less demanding NHCs, for example $iPr_2Im\cdot SbCl_2Mes$ (Scheme 2, **H**).[15] In these isomers the coordination site of the NHC ligand changes from an equatorial (**H**) into an axial position (**G**). We also demonstrated previously that $cAAC^{Me}\cdot SbCl_2Ph$ (Scheme 2, **I**) adopts a stable *Lewis* acid/base adduct which features a solid-state structure similar to compound **H**. Herein we wish to report the different behavior on the reaction of two cAACs with $SbCl_2Mes$, which leads to a convenient synthesis of cAAC-stabilized stibinidenes cAAC·SbMes (Scheme 3).

The reaction of $cAAC^{Me}$ and $cAAC^{Cy}$ with $SbCl_2Mes$ in toluene at −78 °C leads to a pale-yellow slurry, which changes its color to orange-red upon raising the temperature to room temperature. Filtration of the resulting suspensions from a solvent mixture of hexane and toluene (ca. 3:1) separated a colorless precipitate, which consisted of the antimony(III) salts $[cAAC^{Me}Cl][SbCl_3Mes]$ **1a** and $[cAAC^{Cy}Cl][SbCl_3Mes]$ **1b**, respectively. The orange filtrate contained the cAAC-stabilized stibinidenes $cAAC^{Me}\cdot SbMes$ **2a** and $cAAC^{Me}\cdot SbMes$ **2b**, respectively. The latter compounds **2a** and **2b** were readily soluble in *n*-hexane and were isolated as orange solids in 44% and 32% yield. However, these conversions were quantitative if the reaction was performed on NMR scale. All reaction products were characterized by ^1H NMR and $^{13}C\{^1H\}$ NMR spectroscopy, X-ray diffraction analysis and elemental analysis. The characteristic resonances in the ^1H NMR spectrum of **1a** (CH_2, 2.67 ppm; *i*Pr-*CH*, 2.46 ppm) and **1b** (CH_2, 2.66 ppm; *i*Pr-*CH*, 2.46 ppm) revealed almost identical chemical shifts for the $[cAAC^{Me}Cl]^+$ cation as reported previously for the gold salt $[cAAC^{Ad}Cl][AuCl_4]$ (CH_2, 2.67 ppm; *i*Pr-*CH*, 2.45 ppm) of the related *N*-adamantyl substituted cation. The $^{13}C\{^1H\}$ NMR resonances of the carbon atoms attached to chlorine (former carbene carbon atom) of the [cAAC–Cl] cation of **1a–b** (NCCl: **1a**, 190.6 ppm; **1b**, 189.8 ppm) are very characteristic and were almost identical compared to the resonances reported for $[cAAC^{Ad}Cl][AuCl_4]$ (NCCl: 188.5 ppm).[16]

In addition, the ^1H NMR resonances of the mesityl group of compound **2a** (Mes-*p*-CH_3, 2.20 ppm; Mes-*o*-CH_3, 2.81 ppm; Mes-*CH*, 6.99 ppm) and **2b** (Mes-*p*-CH_3, 2.20 ppm; Mes-*o*-CH_3, 2.82 ppm; Mes-*CH*, 6.99 ppm) at the antimony center revealed a clear downfield shift compared to the starting material $SbCl_2Mes$ (Mes-*p*-CH_3, 1.94 ppm; Mes-*o*-CH_3, 2.35 ppm; Mes-*CH*, 6.55 ppm). Furthermore, the characteristic septet of the cAAC methine protons (**2a**, *i*Pr-*CH*, 3.05 ppm; **2b**, *i*Pr-*CH*, 3.06 ppm) is shifted compared to either the free carbene ($cAAC^{Me}$: *i*Pr-*CH*, 3.13 ppm; $cAAC^{Cy}$: *i*Pr-*CH*, 3.15 ppm) or to the *Lewis* acid/base adduct $cAAC^{Me}\cdot SbCl_2Ph$ (*i*Pr-*CH*, 3.25 ppm).[15] The $^{13}C\{^1H\}$ NMR resonances of the carbene carbon atom at 238.7 ppm and 239.4 ppm were also indicative for the formation of the cAAC-stabilized stibinidenes **2a** and **2b** (*cf.* $cAAC^{Cy}\cdot SbCl$: 205.6 ppm in toluene-d_8,[11] $DAC^{Mes}\cdot SbPh$: 205.6 ppm, C_6D_6)[12]). These resonances were remarkably shifted compared to free carbene ($cAAC^{Me}$: 313.6 ppm, and $cAAC^{Cy}$: 316.2 ppm)., and also in a different region as compared to the chlorostibane(III) adduct $cAAC^{Me}\cdot SbCl_2Ph$ (225.8 ppm).[15]

Single crystals of **1a** and **1b** (see Figure 1) suitable for X-ray diffraction analysis were obtained by slow evaporation of a saturated solution of these salts in dichloromethane at room temperature. The compounds **2a** and **2b** (Figure 2) were crystallized by storing at room temperature saturated solutions of these compounds in hexane at −30 °C. The compounds crystallize in the monoclinic space group $P2_1/n$ (**1** and **1b**) and in the triclinic space group $P\bar{1}$ (**2a** and **2b**), respectively, with one molecule in the asymmetric unit. The solid-state structures of **1a** and **1b** (Figure 1) feature separated $[cAAC–Cl]^+$ cations and $[SbCl_3Mes]^-$ counterions, the latter adopt disphenoidal geometries at the antimony(III) center. The antimony atom is substituted by two chlorine atoms in axial positions and a chlorine atom and the mesityl ligand in equatorial position.

The molecular structures of the cAAC-stabilized stibinidenes **2a** and **2b** (Figure 2) reveal two-coordinated antimony(I) atoms in which the cAAC and the mesityl substituent are bent with a C1–Sb–C2 angle of 100.82(9)°

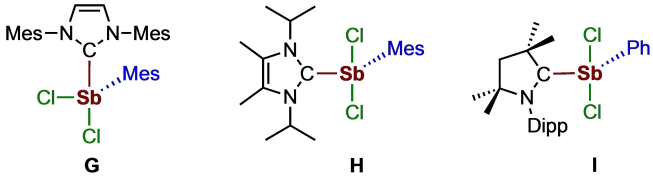

Scheme 2. Isomers of $NHC\cdot SbCl_2Ar$: $Dipp_2Im\cdot SbCl_2Mes$ (**G**), $iPr_2Im^{Me}\cdot SbCl_2Mes$ (**H**), and $cAAC^{Me}\cdot SbCl_2Ph$ (**I**)

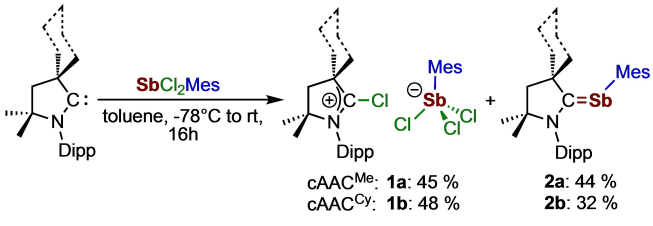

Scheme 3. The reaction of cAACs with $SbCl_2Mes$: Synthesis of the salts $[cAAC^{Me}Cl][SbCl_3Mes]$ (**1a**) and $[cAAC^{Cy}Cl][SbCl_3Mes]$ (**1b**), and the cAAC-stabilized stibinidenes $cAAC^{Me}\cdot SbMes$ (**2a**) and $cAAC^{Cy}\cdot SbMes$ (**2b**). Yields are based on a maximum of 50% for **1** and 50% for **2**.

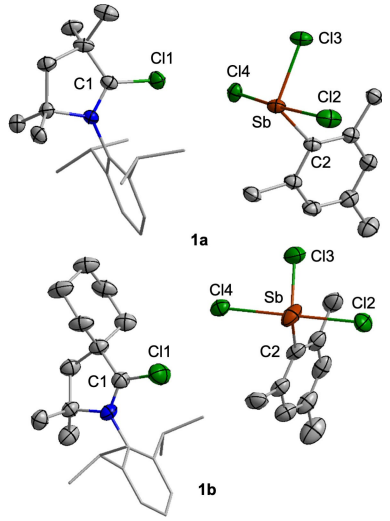

Figure 1. Molecular structures of [cAAC^{Me}Cl][$SbCl_3Mes$] (**1 a**) and [cAAC^{Cy}Cl][$SbCl_3Mes$] (**1 b**) in the solid-state. Hydrogen atoms were omitted for clarity. For **1 a**, the chlorine atom Cl4 is disordered over two sites and the data reported correspond to the part resolved with 86 % occupancy. For **1 b**, the "$SbCl_3$"-unit is disordered over two sites and the data reported correspond to the part with 72 % occupancy. Atomic displacement ellipsoids were set at the 50 % probability level. Selected bond lengths [Å] and angles [°]: **1 a**: C1–Cl1, 1.659(3); Sb–C2, 2.159(2); Sb–Cl2, 2.5514(7); Sb–Cl3, 2.3766(6); Sb–Cl4, 2.4642(8), C2–Sb–Cl2, 89.00(7); C2–Sb–Cl3, 105.80(7); C2–Sb–Cl4, 82.30(8); Cl2–Sb–Cl3, 82.30(8); Cl3–Sb–Cl4, 84.73(3); Cl2–Sb–Cl4, 168.61(5); **1 b**: C1–Cl1, 1.679(5); Sb–C2, 2.183(5); Sb–Cl2, 2.594(6); Sb–Cl3, 2.225(3); Sb–Cl4, 2.612(8), C2–Sb–Cl2, 90.4(2); C2–Sb–Cl3, 110.49(16); C2–Sb–Cl4, 87.6(2); Cl2–Sb–Cl3, 95.16(19); Cl3–Sb–Cl4, 83.8(2); Cl2–Sb–Cl4, 177.2(3).

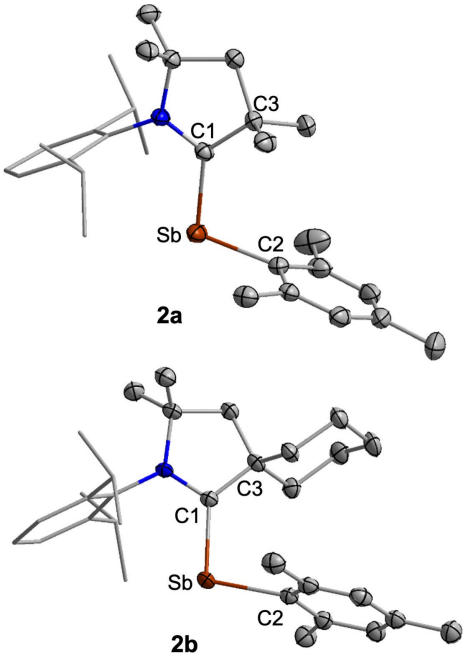

Figure 2. Molecular structures of cAAC^{Me}·SbMes (**2 a**) and cAAC^{Cy}·SbMes (**2 b**) in the solid-state. Hydrogen atoms were omitted for clarity. Atomic displacement ellipsoids were set at the 50 % probability level. Selected bond lengths [Å] and angles [°]: **2 a**: Sb–C1, 2.081(2); Sb–C2, 2.181(2); C1–Sb–C2, 100.82(9); C3–C1–Sb–C2, 4.03(21). **2 b**: Sb–C1, 2.077(3); Sb–C2, 2.186(3); C1–Sb–C2, 100.72(11); C3–C1–Sb–C2, 14.34(30).

(**2 a**) and 100.72(11)° (**2 b**), respectively. The C3–C1–Sb–C2 torsion angle of **2 a** (4.03(21)°) indicates planarity at the antimony center, whereas the structure of **2 b** shows a slightly more distorted alignment with a torsion angle C3–C1–Sb–C2 of 14.34(30)°. This distortion is most probably due to the higher steric demand of cAAC^{Cy} compared to cAAC^{Me}. The Sb–C1 distances of 2.081(2) Å (**2 a**) and 2.077(3) Å (**2 b**) as well as the small distortion angles C3–C1–Sb–C2 at the Sb–C1 bond resembles those of other known stibaalkenes[17] as well as carbene stabilized stibinidenes,[11,12] which feature antimony carbon double bond character. To gain some insight into the bonding situation of **2 a** and **2 b**, we investigated the electronic structure of **2 a** by using DFT calculations at the M06-2X/D3(BJ)//def2-TZVP(Sb)/def2-SVP(C,H,N,Cl)-level of theory. Geometry-optimized **2 a** (Figure 3) closely resembles the essential features of the cAAC-stabilized stibinidene, as was found in the X-ray crystal structure of this compound, with a computed Sb–C1 distance of 2.077 Å (*cf.* exp: 2.081(2) Å), a C1–Sb–C2 angle of 100.1° (exp. 100.82(9)°), and a torsion angle C3–C1–Sb–C2 of 7.2° (4.03(21)°).

Calculations of the relevant orbital energies revealed that the HOMO (Figure 3, **L**) is a Sb=C π-orbital located at the antimony(I) center, and the LUMO is the corresponding π-antibonding orbital. The Wiberg bond index calculated for the Sb=C(cAAC) bond is 1.389 ($d_{Sb\text{-}C}$ = 2.077 Å), much larger than the Wiberg bond index of 0.902 calculated for the Sb–C(Mes) bond ($d_{Sb\text{-}C}$ = 2.183 Å) or 0.713 calculated for cAAC^{Me}·$SbCl_2Mes$ ($d_{Sb\text{-}C(cAAC)}$ = 2.390 Å), which accounts for significant Sb=C(cAAC) double bond character. The HOMO-1 is distributed over the mesityl stibinidene unit with some localization at antimony and can thus be considered as a lone pair located at antimony.

Based on the isolated products and the experience we gathered on carbene adducts of antimony chlorides,[15] a mechanism was proposed for the reaction of cAAC^{Me} with $SbCl_2Mes$ (Scheme 4). In an initial step a *Lewis* acid/base adduct is formed between the *Lewis* base cAAC and *Lewis*-acidic $SbCl_2Mes$ to yield an adduct cAAC^{Me}·$SbCl_2Mes$. This adduct most probably adopts a structure in which the cAAC and one of the chloride substituents occupy axial positions, leading to a partially dissociated chloride substituents in *trans*-position to the excellent donor cAAC.[19] We have demonstrated previously on several occasions that these partially dissociated substituents can be easily transferred to *Lewis* acids.[15,19] The Lewis acid used here is $SbCl_2Mes$, and chloride transfer from cAAC^{Me}·$SbCl_2Mes$ to $SbCl_2Mes$ should form a contact ion pair [cAAC^{Me}·SbClMes][$SbCl_3Mes$] (**3**). The next step is chlorine abstraction from the cationic part of **3**, either by simple chloride transfer to the carbene carbon atom of the cAAC or by cAAC addition to cationic [cAAC^{Me}·SbClMes]$^+$ and subsequent elimi-

Journal of Inorganic and General Chemistry
ZAAC
Zeitschrift für anorganische und allgemeine Chemie

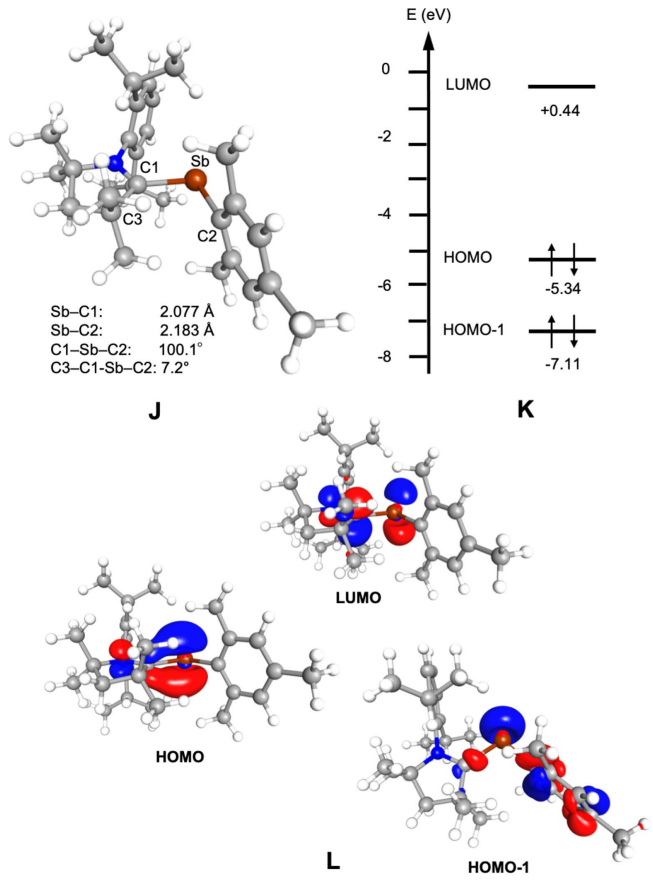

Figure 3. DFT-optimized (M06-2X/D3(BJ)//def2-TZVP(Sb)/def2-SVP(rest)) geometry of cAAC^{Me}·SbMes **2 a** (**J**), orbital energies (**K**) and frontier orbitals (**L**) of **2 a**.

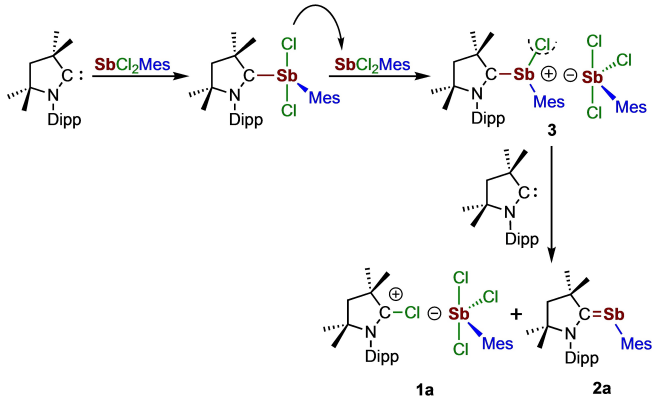

Scheme 4. Proposed mechanism for the formation of the compounds **1 a** and **2 a**.

nation of [cAAC^{Me}Cl]$^-$, which leads to formation of the cAAC-stabilized stibinidene cAAC^{Me}·SbMes (**2 a**) and the salt [cAAC^{Me}Cl][SbCl$_3$Mes] (**1 a**). According to these steps, the reduction of the intermediate cAAC·SbCl$_2$Mes initially formed to yield cAAC·SbMes is accomplished by (i) transfer of "Cl$^-$" from cAAC·SbCl$_2$Mes to SbCl$_2$Mes (second step in Scheme 4) and (ii) formal transfer of "Cl$^+$" from [cAAC^{Me}·SbClMes]$^+$ to the cAAC, which makes in total the carbene carbon atom of cAAC^{Me} the reducing reagent. The mechanism involving the addition of cAAC^{Me} and subsequent elimination of [cAAC^{Me}Cl]$^+$ could be regarded as a reductive elimination at a main group element center.[20]

To support this mechanism, we reacted two equivalents SbCl$_2$Mes with only one equivalent of cAAC^{Me} in the hope to prevent the last step (i.e. "Cl$^+$" transfer). To our delight, if the reaction was performed in benzene at room temperature, compound **3** crystallized in low yield from the reaction mixture of the sluggish reaction. This salt crystallizes in the monoclinic space group P2$_1$/c with one molecule in the asymmetric unit. The solid-state structure of **3** (Figure 4) reveals the salt [cAAC^{Me}·SbClMes]$^+$[SbCl$_3$Mes]$^-$, in which the cation [cAAC^{Me}·SbClMes]$^+$ adopts a three-coordinate pyramidal structure and the [SbCl$_3$Mes]$^-$ anion a four-coordinate disphenoidal geometry. The Sb1–C1 distance to the cAAC ligand of 2.258(3) Å is in the range of Sb–C distances observed previously for carben adducts of antimony(III) chlorides, for example 2.239(2) Å in cAAC^{Me}·SbCl$_3$ or 2.243(3) Å in cAAC^{Me}·SbCl$_2$Ph,[15] and is in line with a C–Sb single bond. Furthermore, it is worthy to note that the NCSb ^{13}C{^{1}H} NMR resonance of **3** at 231.2 ppm (CD$_2$Cl$_2$) is located in-between the resonances observed for cAAC^{Me}·SbCl$_2$Ph (225.8 ppm) and for the stibinidenes **2 a** and **2 b** (**2 a**, 238.7 ppm; **2 b**, 239.4 ppm; C$_6$D$_6$). The isolation of compound **3** thus strongly supports the mechanism proposed in Scheme 4.

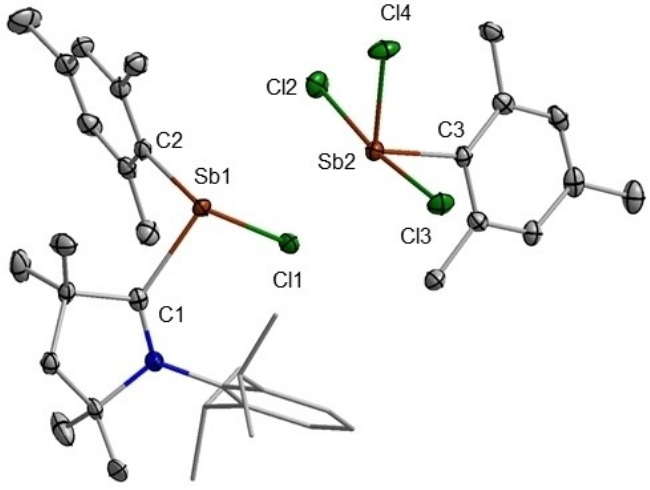

Figure 4. Molecular structure of [cAAC^{Me}·SbClMes][SbCl$_3$Mes] (**3**) in the solid-state. Hydrogen atoms and solvent molecules (benzene) were omitted for clarity. The "SbCl" unit in the [cAAC^{Me}·SbClMes]$^+$ cation is disordered over two sites and the data corresponding to the part with 93 % occupancy is shown. Atomic displacement ellipsoids were set at the 50 % probability level. Selected bond lengths [Å] and angles [°]: **3**: Sb1–C1, 2.258(3); Sb1–C2, 2.164(3); Sb1–Cl1, 2.3614(8); Sb2–C3, 2.161(3); Sb2–Cl2, 2.5898(7); Sb2–Cl3, 2.6285(7); Sb2–Cl4, 2.3742(7); C1–Sb1–C2, 96.44(10); C1–Sb–Cl1, 98.69(7); C2–Sb–Cl1, 101.24(8); Cl2–Sb2–C3, 89.27(7); Cl2–Sb2–Cl3, 172.78(2); Cl2–Sb2–Cl4, 88.05(2); Cl3–Sb2–C3, 89.17(7); Cl3–Sb2–Cl4, 85.57(2); Cl4–Sb–C3, 105.36(7).

In conclusion, we report herein the quantitative synthesis of the cAAC-stabilized stibinidenes cAAC^{Me}·SbMes (**2 a**) and cAAC^{Cy}·SbMes (**2 b**) starting from $SbCl_2Mes$ and cAAC, which is accompanied with the 50% formation of the salts [cAAC^{Me}Cl][$SbCl_3Mes$] (**1 a**) and [cAAC^{Cy}Cl][$SbCl_3Mes$] (**1 b**). The compounds were characterized by NMR- and IR spectroscopy, elemental analysis, and X-ray diffraction analysis. The bonding situation of **2 a** was examined in some detail with the aid of DFT calculations, which accounts for an antimony carbene carbon double bond. A mechanism was proposed for this reaction which explains the reduction of the intermediate cAAC·$SbCl_2Mes$ initially formed with the cAAC carbene carbon atom to yield cAAC·SbMes (**2 a**), i.e. the cAAC is used as the reducing reagent with oxidation of the carbene carbon atom. The important intermediate [cAAC^{Me}·SbClMes][$SbCl_3Mes$] (**3**) of this reaction sequence was isolated and structurally characterized. The procedure presented here is a convenient synthesis of cAAC-stabilized stibinidenes although one equivalent of cAAC and one equivalent of antimony is lost. We failed so far in the metallic reduction of **1**, which should – in principle – also afford cAAC-stabilized stibinidenes **2**. We also failed so far to replace $SbCl_2Mes$ as *Lewis*-acidic chloride acceptor, mainly because of the formation of stable adducts of the Lewis acids then employed with the cAAC. However, the beauty of this reaction lies in a 100% conversion and the ease of the separation of **1** and **2**, which makes the further exploration of the chemistry of cAAC-stabilized stibinidenes convinient.

Experimental Section

General Procedure

All reactions and subsequent manipulations involving organometallic reagents were performed under an argon atmosphere by using standard Schlenk techniques or in a Glovebox (Innovative Technology Inc. and MBraun Uni Lab) as reported previously.[21] All reactions were carried out in oven-dried glassware. Toluene, *n*-hexane and THF were obtained from a solvent purification system (Innovative Technology). Deuterated solvents were purchased from Sigma-Aldrich and stored over molecular sieves (4 Å). $SbCl_2Mes$[22] and cAAC[23] were prepared according to literature procedures. All other reagents were purchased from Sigma-Aldrich or ABCR and used without further purification. Elemental analyses were performed in the micro-analytical laboratory of the University of Würzburg with an Elementar vario micro cube. NMR spectra were recorded at 298 K using Bruker Avance 400 (^{1}H: 400.4 MHz; ^{13}C{^{1}H}: 100.7 MHz) or Bruker Avance 500 (^{1}H: 500.1 MHz; ^{13}C{^{1}H}: 125.8 MHz) NMR spectrometers. Assignment of the ^{1}H NMR spectra was supported by ^{1}H,^{1}H and ^{13}C{^{1}H},^{1}H correlation experiments. ^{13}C NMR spectra were broadband proton-decoupled (^{13}C{^{1}H}). Assignment of the ^{13}C NMR data was supported by ^{13}C{^{1}H},^{1}H correlation experiments. ^{1}H and ^{13}C{^{1}H} NMR chemical shifts are listed in parts per million (ppm) and were referenced *via* residual proton resonances of the corresponding deuterated solvent (C_6D_5H (^{1}H: $\delta = 7.16$, C_6D_6), $CDHCl_2$ (^{1}H: $\delta = 5.32$, CD_2Cl_2)). ^{13}C NMR spectra are reported relative to the carbon resonances of the deuterated solvents C_6D_6 (^{13}C: $\delta = 128.06$), CD_2Cl_2 (^{13}C: $\delta = 53.84$) which were referenced to TMS.[24] Coupling constants are quoted in Hertz. Infrared spectra were recorded on solid samples at room temperature on a Bruker Alpha FT-IR spectrometer using an ATR unit and are reported in cm^{-1}. In dependence of the intensity of the vibration bands the following abbreviations were used: very strong (vs), strong (s), middle (m), weak (w) and very weak (vw).

Synthesis of [cAAC^{Me}Cl][$SbCl_3Mes$] (1 a) and cAAC^{Me}·SbMes (2 a)

A solution of $SbCl_2Mes$ (983 mg, 3.15 mmol, 1 eq) in toluene (22 mL) was added under vigorous stirring at −78 °C to a solution of cAAC^{Me} (106 mg, 371 μmol, 1 eq) in toluene (22 mL). The suspension was stirred for three hours at −78 °C with subsequent warming to room temperature over 17 hours. The orange-red suspension was concentrated to a volume of 15 mL and hexane (50 mL) was added. The resulting suspension was filtered and washed with *n*-hexane (2×15 mL) to yield **1 a** (949 mg, 1.42 mmol, 45%) as an off-white solid. Crystals of **1 a** suitable for X-ray diffraction analysis were grown by slow evaporation of a saturated solution of the compound in dichloromethane at room temperature. Removal of all volatile material of the filtrate afforded **2 a** (722 mg, 1.37 mmol, 44%) as an orange solid. However, it was found that such good yields could only be obtained if these conditions were strictly kept, otherwise increased decomposition was observed. In some instances, the product had to be recrystallized for further purification by storing a saturated and filtrated hexane solution of the compound at −30 °C for several days. These crystals are typically also suitable for X-ray diffraction analysis.

[cAAC^{Me}Cl][$SbCl_3Mes$] (1 a): ^{1}H NMR (400.5 MHz, CD_2Cl_2, 298 K): δ [ppm] = 1.19 (d, 6 H, $^3J_{HH}$ = 6.8 Hz, *i*Pr-CH_3), 1.38 (d, 6 H, $^3J_{HH}$ = 6.8 Hz, *i*Pr-CH_3), 1.59 (s, 6 H, NC(CH_3)$_2$), 1.71 (s, 6 H, NCC(CH_3)$_2$), 2.22 (s, 3 H, Mes-*p*-CH_3), 2.46 (sept, 2 H, $^3J_{HH}$ = 6.8 Hz, *i*Pr-C*H*), 2.67 (s, 2 H, CH_2), 2.71 (s, 6 H, Mes-*o*-CH_3), 6.82 (s, 2 H, Mes-C*H*), 7.46 (d, 2 H, $^3J_{HH}$ = 7.8 Hz, Dipp-*m*-C*H*), 7.67 (t, 1 H, $^3J_{HH}$ = 7.8 Hz, Dipp-*p*-C*H*). **^{13}C{^{1}H} NMR** (100.7 MHz, CD_2Cl_2, 298 K): δ [ppm] = 21.1 (Mes-*p*-CH_3), 22.5 (Mes-*o*-CH_3), 23.4 (*i*Pr-CH_3), 26.3 (*i*Pr-CH_3), 28.3 (NC(CH_3)$_2$), 28.9 (NCC(CH_3)$_2$), 30.4 (*i*Pr-C*H*), 48.0 (CH_2), 51.6 (NC(CH_3)$_2$), 84.4 (NC(CH_3)$_2$), 126.9 (Mes-*m*-C*H*), 127.6 (Dipp-*i*-*C*), 130.3 (Dipp-*m*-C*H*), 133.2 (Dipp-*p*-C*H*), 138.6 (Mes-*p*-*C*), 143.0 (Mes-*o*-*C*), 144.7 (Dipp-*o*-*C*), 155.2 (Mes-*i*-*C*), 190.6 (NCCl). **Elemental analysis** (%) calcd. for $C_{29}H_{42}Cl_4NSb$ [668.22 g/mol]: C, 52.13; H, 6.34; N, 2.10; found: C, 52.33; H, 6.39; N, 2.01. **IR** ([cm^{-1}]): 3005 (vw), 2973 (m), 2931 (m), 2867 (w), 1644 (vw), 1602 (s) 1582 (w), 1463 (s), 1454 (s), 1391 (m), 1384 (m), 1372 (m), 1346 (w), 1336 (w), 1287 (w), 1265 (m), 1202 (w), 1178 (w), 1164 (w), 1133 (s), 1108 (m), 1061 (m), 1052 (m), 1034 (m), 969 (vw), 933 (w), 910 (vw), 890 (w), 868 (w), 848 (m), 808 (vs), 793 (m), 765 (vw), 737 (m), 704 (w), 652 (vw), 630 (vw), 609 (vw), 577 (w), 563 (w), 543 (w), 493 (w), 425 (vw), 416 (vw).

cAAC^{Me}·SbMes (2 a): ^{1}H NMR (500.1 MHz, C_6D_6, 298 K): δ [ppm] = 1.05 (s, 6 H, NCC(CH_3)$_2$), 1.24 (d, 6 H, $^3J_{HH}$ = 6.8 Hz, *i*Pr-CH_3), 1.28 (s, 6 H, NC(CH_3)$_2$), 1.69 (s, 2 H, CH_2), 1.77 (d, 6 H, $^3J_{HH}$ = 6.8 Hz, *i*Pr-CH_3), 2.20 (s, 3 H, Mes-*p*-CH_3), 2.81 (s, 6 H, Mes-*o*-CH_3), 3.05 (sept, 2 H, $^3J_{HH}$ = 6.8 Hz, *i*Pr-C*H*), 6.99 (s_{br}, 2 H, Mes-C*H*), 7.159 (d, 1 H, $^3J_{HH}$ = 8.4 Hz, Dipp-*m*-C*H*, overlapped with C_6D_5H), 7.160 (d, 1 H, $^3J_{HH}$ = 6.9 Hz, Dipp-*m*-C*H*, overlapped with C_6D_5H), 7.67 (dd, 1 H, $^3J_{HH}$ = 6.9 Hz, $^3J_{HH}$ = 8.4 Hz, Dipp-*p*-C*H*). **^{13}C{^{1}H} NMR** (125.8 MHz, C_6D_6, 298 K): δ [ppm] = 21.2 (Mes-*p*-CH_3), 25.3 (*i*Pr-CH_3), 28.8 (*i*Pr-CH_3), 29.0 (*i*Pr-C*H*), 29.1 (NCC(CH_3)$_2$), 31.0 (NC(CH_3)$_2$), 31.3 (Mes-*o*-CH_3), 55.7 (CH_2), 55.9 (NC(CH_3)$_2$) 71.5 (NCC(CH_3)$_2$), 126.4 (Dipp-*m*-C*H*), 127.6 (Mes-*m*-C*H*), 129.4 (Dipp-*p*-C*H*), 136.1 (Dipp-*i*-*C*), 137.3 (Mes-*p*-*C*), 138.5 (Mes-*i*-*C*), 146.2 (Mes-*o*-*C*), 148.0 (Dipp-*o*-*C*), 238.6 (NCSb). **Elemental analysis** (%) calcd. for $C_{29}H_{42}NSb$ [526.42 g/mol]: C, 66.17; H, 8.04; N, 2.66; found: C, 66.40; H, 8.17; N, 2.54. **IR** ([cm^{-1}]): 3058 (vw), 2960 (s), 2926 (s), 2864 (m), 1678 (m), 1590 (vw), 1441 (m), 1382 (m), 1366 (m),

1336 (vs), 1254 (m), 1234 (w), 1203 (s), 1178 (m), 1137 (s), 1109 (m), 1050 (m), 1012 (m), 975 (w), 957 (w), 939 (m), 899 (w), 847 (m), 805 (s), 776 (m), 751 (w), 698 (w), 638 (vw), 608 (vw), 574 (m), 550 (w), 540 (w), 479 (vw), 447 (w), 431 (vw), 408 (vw).

Synthesis of [cAAC^{Cy}Cl][SbCl$_3$Mes] (1 b) and cAAC^{Cy}·SbMes (2 b)

A solution of $SbCl_2Mes$ (192 mg, 614 μmol, 1 eq) in toluene (7 mL) was added under vigorous stirring at −78 °C to a solution of cAAC^{Cy} (200 mg, 614 μmol, 1 eq) in toluene (7 mL). The suspension was stirred for three hours at −78 °C with subsequent warming to room temperature over 17 hours. The orange suspension was concentrated to a volume of 5 mL and hexane (15 mL) was added. The resulting suspension was filtered and washed with *n*-hexane (3× 10 mL) to yield **1 b** (211 mg, 298 μmol, 48 %) as an off-white solid. In some instances, the product had to be purified by slow diffusion of n-hexane into a saturated solution of the compound in THF at room temperature which afforded **1 b** (46.0 mg, 65.0 μmol, 11 %) as a colorless crystalline solid. These crystals were also suitable for X-ray diffraction analysis. Removal of all volatile material of the filtrate afforded **2 b** (126 mg, 198 μmol, 32 %) as an orange solid. It was found that such good yields could only be obtained if the conditions mentioned here were strictly kept, otherwise increased decomposition was observed. In some instances, the product had to be recrystallized for further purification by storing a saturated and filtrated solution of the compound in hexane at −30 °C for several days. These crystals of **2 b** were also suitable for X-ray diffraction analysis.

cAAC^{Cy}Cl][SbCl$_3$Mes] (1 b): ^{1}H NMR (400.5 MHz, CD_2Cl_2, 258 K): δ [ppm] = 1.18 (d, 6 H, $^3J_{HH}$ = 6.7 Hz, *i*Pr-CH_3), 1.38 (d, 6 H, $^3J_{HH}$ = 6.7 Hz, *i*Pr-CH_3), 1.40 (m, 1 H, Cy-CH_2), 1.50 (m, 2 H, Cy-CH_2), 1.59 (s, 6 H, NC(CH_3)$_2$), 1.86 (m, 2 H, Cy-CH_2), 1.97 (m, 4 H, Cy-CH_2, overlapped with m, 1 H, Cy-CH_2), 2.23 (s, 3 H, Mes-*p*-CH_3), 2.46 (sept, 2 H, $^3J_{HH}$ = 6.7 Hz, *i*Pr-C*H*), 2.66 (s, 2 H, CH_2), 2.71 (s, 6 H, Mes-*o*-CH_3), 6.82 (s, 2 H, Mes-C*H*), 7.46 (d, 2 H, $^3J_{HH}$ = 7.8 Hz, Dipp-*m*-C*H*), 7.65 (t, 1 H, $^3J_{HH}$ = 7.8 Hz, Dipp-*p*-C*H*). **^{13}C{^{1}H} NMR** (100.7 MHz, CD_2Cl_2, 298 K): δ [ppm] = 21.1 (Mes-*p*-CH_3), 21.4 (Cy-CH_2 overlapped with Cy-CH_2), 22.6 (Mes-*o*-CH_3), 23.4 (*i*Pr-CH_3), 24.5 (Cy-CH_2), 26.3 (*i*Pr-CH_3), 29.4 (NCCH_3)$_2$), 30.4 (*i*Pr-CH), 35.8 (Cy-CH_2), 44.1 (CH_2), 56.3 (NCCCy), 83.8 (NC(CH$_3$)$_2$), 126.9 (Mes-*m*-CH), 127.6 (Dipp-*i*-C), 130.3 (Dipp-*m*-CH), 133.1 (Dipp-*p*-CH), 138.7 (Mes-*p*-C), 143.1 (Mes-*o*-C), 144.7 (Dipp-*o*-C), 154.9 (Mes-*i*-C), 189.8 (NCCl). **Elemental analysis** (%) calcd. for $C_{32}H_{46}Cl_4NSb$ [708.26 g/mol]: C, 54.27; H, 6.55; N, 1.98; found: C, 54.07; H, 6.54; N, 1.97. **IR** ([cm^{-1}]): 2969 (m), 2930 (s), 2858 (m), 1724 (vw), 1680 (vw), 1641 (vw), 1600 (s), 1581 (m), 1463 (s), 1446 (vs), 1388 (m), 1374 (m), 1346 (w), 1320 (w), 1288 (w), 1270 (w), 1247(m), 1205 (w), 1180 (w), 1158 (w), 1132 (s), 1118 (m), 1053 (m), 1029 (w), 1014 (w), 991 (vw), 935 (m), 873 (vw), 848 (m), 807 (s), 781 (vw), 765 (vw), 735 (w), 705 (w), 688 (vw), 650 (vw), 630 (vw), 592 (w), 579 (w), 562 (w), 553 (w), 542 (w), 529 (w), 490 (w), 422 (w),

cAAC^{Me}·SbMes (2 b): ^{1}H NMR (400.5 MHz, C_6D_6, 298 K): δ [ppm] = 0.63 (m, 1 H, Cy-CH_2), 1.06 (s, 6 H, NC(CH_3)$_2$), 1.10 (m, 2 H, Cy-CH_2), 1.26 (d, 6 H, $^3J_{HH}$ = 6.7 Hz, *i*Pr-CH_3), 1.14 (m, 1 H, Cy-CH_2 overlapped with m, 1 H, Cy-CH_2), 1.68 (m, 2 H, Cy-CH_2), 1.78 (s, 2 H, CH_2), 1.79 (d, 6 H, $^3J_{HH}$ = 6.7 Hz, *i*Pr-CH_3), 2.02 (m, 2 H, Cy-CH_2) 2.20 (s, 3 H, Mes-*p*-CH_3), 2.82 (s, 6 H, Mes-*o*-CH_3), 3.06 (sept, 2 H, $^3J_{HH}$ = 6.7 Hz, *i*Pr-C*H*), 6.99 (s_{br}, 2 H, Mes-C*H*), 7.17 (d, 1 H, $^3J_{HH}$ = 8.7 Hz, Dipp-*m*-C*H*, overlapped with C_6D_5H), 7.17 (d, 1 H, $^3J_{HH}$ = 6.7 Hz, Dipp-*m*-C*H*, overlapped with C_6D_5H), 7.67 (dd, 1 H, $^3J_{HH}$ = 6.7 Hz, $^3J_{HH}$ = 8.7 Hz, Dipp-*p*-C*H*). **^{13}C{^{1}H} NMR** (125.8 MHz, C_6D_6, 298 K): δ [ppm] = 21.2 (Mes-*p*-CH_3), 23.3 (Cy-CH_2), 25.4 (*i*Pr-CH_3), 25.8 (Cy-CH_2), 28.9 (*i*Pr-CH_3), 29.0 (*i*Pr-CH), 29.6 (NC(CH_3)$_2$), 31.3 (Mes-*o*-CH_3), 37.9 (Cy-CH_2),49.6 (CH_2), 60.9 (NC(CH$_3$)$_2$) 71.9 (NCCCy), 126.4 (Dipp-*m*-CH), 127.6 (Mes-*m*-CH), 129.4 (Dipp-*p*-CH), 136.1 (Dipp-*i*-C), 137.2 (Mes-*p*-C), 139.2 (Mes-*i*-C), 146.1 (Mes-*o*-C), 148.0 (Dipp-*o*-C), 239.4 (NCSb). **Elemental analysis** (%) calcd. for $C_{32}H_{46}NSb$ [566.49 g/mol]: C, 67.85; H, 8.19; N, 2.47; found: C, 67.56; H, 8.33; N, 2.38. **IR** ([cm^{-1}]): 3053 (vw), 2963 (s), 2921 (s), 2861 (m), 1678 (m), 1589 (vw), 1463 (m), 1441 (m), 1382 (m), 1362 (m), 1347 (s), 1336 (vs), 1285(w), 1259 (m), 1241 (m), 1227 (m), 1202 (w), 1175 (s), 1153 (m), 1112 (s), 1096 (s), 1050 (s), 1039 (m), 1015 (m), 933 (m), 889 (w), 846 (m), 805 (vs), 777 (m), 766 (w), 699 (w), 638 (vw), 614 (vw), 600 (vw), 579 (vw), 563 (vw), 549, 530 (vw), 477 (vw), 455 (vw), 430 (vw), 411 (vw).

Synthesis of [cAAC^{Me}·SbClMes][SbCl$_3$Mes] (3)

A mixture of cAAC^{Me} (10.0 mg, 35.0 μmol, 1 eq) and $SbCl_2Mes$ (21.9 mg, 70.1 μmol, 2 eq) was suspended at room temperature in C_6D_6 (0.6 mL). After a few minutes a yellow oil precipitates which contains a mixture of compounds. At the layer between oil and solvent compound **3** crystallizes after 1–3 days. The solvent and residual oil was removed and the crystalline solid was washed with toluene (2×1 mL) to yield **3** (7.60 mg, 1.42 mmol, 24 %) as a colorless crystalline solid. These crystals were suitable for X-ray diffraction analysis.

[cAAC^{Me}·SbClMes][SbCl$_3$Mes] (3): ^{1}H NMR (500.1 MHz, CD_2Cl_2, 258 K): δ [ppm] = 1.05 (br, 6 H, Mes-*p*-CH_3), 1.25 (d, 6 H, $^3J_{HH}$ = 6.3 Hz, *i*Pr-CH_3), 1.61 (s, 6 H, NCC(CH_3)$_2$), 1.72 (s, 6 H, NC(CH_3)$_2$), 2.20 (s, 3 H, Mes-*p*-CH_3), 2.25 (d, 6 H, $^3J_{HH}$ = 6.3 Hz, *i*Pr-CH_3), 2.27 (s, 3 H, Mes-*p*-CH_3), 2.42 (sept, 2 H, $^3J_{HH}$ = 6.3 Hz, *i*Pr-C*H*), 2.49 (s, 2 H, CH_2), 2.66 (s, 6 H, Mes-*o*-CH_3), 6.82 (s, 2 H, Mes-C*H*), 6.98 (s, 2 H, Mes-C*H*), 7.34 (d, 2 H, $^3J_{HH}$ = 7.8 Hz, Dipp-*m*-C*H*), 7.60 (t, 1 H, $^3J_{HH}$ = 7.8 Hz, Dipp-*p*-C*H*). **^{13}C{^{1}H} NMR** (125.8 MHz, CD_2Cl_2, 258 K): δ [ppm] = 20.9 (Mes-*p*-CH_3), 21.0 (*i*Pr-CH_3), 22.2 (Mes-*o*-CH_3), 24.0 (Mes-*o*-CH_3), 26.1 (Mes-*p*-CH_3, overlapped by NCC(CH_3)$_2$), 27.3 (*i*Pr-CH_3), 28.3 (NC(CH_3)$_2$), 29.4 (*i*Pr-CH), 52.9 (CH_2), 57.9 (NCC(CH_3)$_2$), 86.1 (NC(CH_3)$_2$), 127.3 (Dipp-*m*-CH), 129.9 (Mes-CH_2), 130.2 (Mes-CH_2), 131.7 (Dipp-*i*-C), 132.8 (Dipp-*p*-C), 138.7 (Mes-*p*-C), 140.7 (Mes-*i*-C), 142.6 (Mes-*o*-C), 143.6 (Mes-*p*-C), 144.1 (Dipp-*o*-C), 144.9 (Dipp-*o*-C), 153.4 (Mes-*i*-C), 231.2 (NCSb). **Elemental analysis** (%) calcd. for $C_{38}H_{53}Cl_4NSb_2$ + (C_6H_6) [987.28 g/mol]: C, 53.53; H, 6.02; N, 1.42; found: C, 53.14; H, 5.96; N, 1.35. **IR** ([cm^{-1}]): 3002 (vw), 2967 (m), 2927 (w), 2867 (w), 1644 (vw), 1595 (w), 1555 (vw), 1526 (w), 1458(m), 1447 (m), 1389 (w), 1373 (m), 1329 (w), 1312 (vw), 1292 (w), 1265 (vw), 1242 (vw), 1203 (vw), 1181 (w), 1121 (w), 1106 (w), 1089 (vw), 1049 (w), 1030 (w), 1010 (vw), 971 (vw), 927 (vw), 874 (vw), 852 (m), 807 (s), 770 (m), 737 (vw), 702 (vw), 672 (vw), 630 (vw), 608 (vw), 593 (vw), 580 (w), 563 (w), 553 (w), 541 (w), 504 (vs), 432 (vw).

Crystallographic Details. Crystals were immersed in a film of perfluoropolyether oil on a nylon fiber and transferred to a Bruker D8 Apex-1 diffractometer with CCD area detector and graphite-monochromated Mo-K_α radiation or a Bruker D8 Apex-2 diffractometer with CCD area detector and graphite-monochromated Mo-K_α radiation equipped with an Oxford Cryosystems low-temperature device or a Rigaku XtaLAB Synergy-DW diffractometer with HyPix-6000HE detector and monochromated Cu-K_α equipped with an Oxford Cryo 800 cooling unit. Data were collected at 100 K. The images were processed with the Bruker or Crysalis software packages and equivalent reflections were merged. Corrections for Lorentz-polarization effects and absorption were performed if necessary and the structures were solved by direct methods. Subsequent difference Fourier syntheses revealed the positions of all other non-hydrogen atoms. The structures were solved by using the ShelXTL software package.[25] All non-hydrogen atoms were refined anisotropically. Hydrogen atoms were usually assigned to idealized positions and were included in structure factors calculations. Crystallographic data

for the structures reported in this paper have been deposited with the Cambridge Crystallographic Data Centre as supplementary publication no.s CCDC 2154795 (**1 a**), CCDC 2154792 (**1 b**), CCDC 2154796 (**2 a**), CCDC 2154793 (**2 b**), CCDC 2154794 (**3**).

Crystal Data for [cAAC^{Me}Cl][SbCl$_3$Mes] (1 a): $C_{29}H_{42}Cl_4NSb$, M_r = 668.18, T = 100(2) K, λ = 1.54184 Å, colorless block, 0.123×0.077×0.052 mm^3, monoclinic space group $P2_1/n$ = 13.78960(10) Å, b = 13.02660(10) Å, c = 17.52970(10) Å, α = 90°, β = 96.7180(10)°, γ = 90°, V = 3127.27(4) Å^3, Z = 4, ρ_{calcd} = 1.419 Mg/m^3, μ = 10.267 mm^{-1}, F(000) = 1368, 125248 reflections, $-17 \le h \le 17$, $-16 \le k \le 16$, $-22 \le l \le 22$, 3.866° < θ < 77.735°, completeness 99.5 %, 6659 independent reflections, 6376 reflections observed with [I > 2σ(I)], 337 parameters, 6 restraints, R indices (all data) R_1 = 0.0324, wR_2 = 0.0859, final R indices [I > 2σ(I)] R_1 = 0.0313, wR_2 = 0.0851, largest difference peak and hole 0.512 and −1.287 eÅ^{-3}, Goof = 1.063.

Crystal Data for [cAAC^{Cy}Cl][SbCl$_3$Mes] (1 b): $C_{32}H_{46}Cl_4NSb$, M_r = 708.26, T = 100(2) K, λ = 1.54184 Å, colorless block, 0.238×0.177×0.133 mm^3, monoclinic space group $P2_1/n$ = 12.7652(4) Å, b = 18.9144(3) Å, c = 14.5524(6) Å, α = 90°, β = 107.298(4)°, γ = 90°, V = 3354.70(19) Å^3, Z = 4, ρ_{calcd} = 1.402 Mg/m^3, μ = 9.603 mm^{-1}, F(000) = 1456, 35514 reflections, $-15 \le h \le 15$, $-21 \le k \le 23$, $-18 \le l \le 17$, 3.948° < θ < 75.951°, completeness 98.1 %, 6860 independent reflections, 5346 reflections observed with [I > 2σ(I)], 389 parameters, 54 restraints, R indices (all data) R_1 = 0.0796, wR_2 = 0.1442, final R indices [I > 2σ(I)] R_1 = 0.0615, wR_2 = 0.1358, largest difference peak and hole 0.899 and −1.093 eÅ^{-3}, Goof = 1.049.

Crystal Data for cAAC^{Me}·SbMes (2 a): $C_{29}H_{42}NSb$, M_r = 526.38, T = 100(2) K, λ = 1.54184 Å, orange block, 0.367×0.212×0.131 mm^3, triclinic space group $P\bar{1}$ = 10.0016(2) Å, b = 10.2416(3) Å, c = 14.7407(4) Å, α = 102.464(2)°, β = 101.608(2)°, γ = 105.992(2)°, V = 1361.53(6) Å^3, Z = 2, ρ_{calcd} = 1.284 Mg/m^3, μ = 8.124 mm^{-1}, F(000) = 548, 50805 reflections, $-12 \le h \le 12$, $-12 \le k \le 12$, $-18 \le l \le 18$, 3.196° < θ < 77.659°, completeness 97.8 %, 5685 independent reflections, 5403 reflections observed with [I > 2σ(I)], 291 parameters, 0 restraints, R indices (all data) R_1 = 0.0326, wR_2 = 0.0833, final R indices [I > 2σ(I)] R_1 = 0.0309, wR_2 = 0.0818, largest difference peak and hole 0.997 and −0.744 eÅ^{-3}, Goof = 1.114.

Crystal Data for cAAC^{Cy}·SbMes (2 b): $C_{32}H_{46}NSb$, M_r = 566.45, T = 100(2) K, λ = 1.54184 Å, orange block, 0.461×0.159×0.109 mm^3, triclinic space group $P\bar{1}$ = 9.0174(2) Å, b = 11.6959(2) Å, c = 14.7708(3) Å, α = 77.915(2)°, β = 73.012(2)°, γ = 82.911(2)°, V = 1453.60(5) Å^3, Z = 2, ρ_{calcd} = 1.294 Mg/m^3, μ = 7.647 mm^{-1}, F(000) = 592, 29808 reflections, $-11 \le h \le 11$, $-12 \le k \le 14$, $-18 \le l \le 18$, 3.182° < θ < 75.196°, completeness 97.1 %, 5846 independent reflections, 5394 reflections observed with [I > 2σ(I)], 316 parameters, 0 restraints, R indices (all data) R_1 = 0.0399, wR_2 = 0.0965, final R indices [I > 2σ(I)] R_1 = 0.0374, wR_2 = 0.0951, largest difference peak and hole 0.877 and −1.966 eÅ^{-3}, Goof = 1.118.

Crystal Data for [cAAC^{Me}SbClMes][SbCl$_3$Mes] (3): $C_{38}H_{36}Cl_4NSb_2$, (C_6H_6), M_r = 987.24, T = 100(2) K, λ = 0.71073 Å, red block, 0.149×0.131×0.068 mm^3, monoclinic space group $P2_1/c$ = 16.1062(4) Å, b = 12.8290(3) Å, c = 90°, β = 108.097(3)°, γ = 90°, V = 4398.9(2) Å^3, Z = 4, ρ_{calcd} = 1.491 Mg/m^3, μ = 1.502 mm^{-1}, F(000) = 2000, 66967 reflections, $-22 \le h \le 22$, $-17 \le k \le 17$, $-31 \le l \le 28$, 1.913° < θ < 29.575°, completeness 100 %, 12328 independent reflections, 9175 reflections observed with [I > 2σ(I)], 493 parameters, 22 restraints, R indices (all data) R_1 = 0.0616, wR_2 = 0.0761, final R indices [I > 2σ(I)] R_1 = 0.0349, wR_2 = 0.0675, largest difference peak and hole 1.122 and −2.666 eÅ^{-3}, Goof = 1.013.

Computational Details. The calculations were carried out using the TURBOMOLE V7.5.1 suite of programs.[26] Geometry optimizations were performed using (RI-)DFT calculations[27] on a m4 grid employing the D3BJ[28] dispersion-corrected M06-2x[29] functional and a def2-TZVP basis set for Sb and def2-SVP basis sets for C, H, N and Cl atoms.[30] Wiberg bond indices[31] have been evaluated from the DFT ground state electron density.

Acknowledgements

This work was supported by the Julius-Maximilians-Universität Würzburg and the Deutsche Forschungsgemeinschaft (RA720/13). Open Access funding enabled and organized by Projekt DEAL.

Conflict of Interest

The authors declare no conflict of interest.

Data Availability Statement

The data that support the findings of this study are available in the supplementary material of this article.

Keywords: Antimony · Cyclic (alkyl)(amino)carbenes · *Lewis* acid/base adducts · Main group element halides · Stibinidenes

[1] a) W. A. Herrmann, C. Köcher, *Angew. Chem.* **1997**, *109*, 2256–2282; *Angew. Chem. Int. Ed.* **1997**, *36*, 2162–2187; b) D. Bourissou, O. Guerret, F. P. Gabbaï, G. Bertrand, *Chem. Rev.* **2000**, *100*, 39–91; c) S. P. Nolan, N-Heterocyclic Carbenes in Synthesis; Wiley-VCH, Weinheim, Germany, 2006; d) F. E. Hahn, M. C. Jahnke, *Angew. Chem.* **2008**, *120*, 3166–3216; *Angew. Chem. Int. Ed.* **2008**, *47*, 3122–3172; e) T. Dröge, F. Glorius, *Angew. Chem.* **2010**, *122*, 7094–7107; *Angew. Chem. Int. Ed.* **2010**, *49*, 6940–6952; f) M. N. Hopkinson, C. Richter, M. Schedler, F. Glorius, *Nature* **2014**, *510*, 485–496.

[2] a) M. Melaimi, M. Soleilhavoup, G. Bertrand, *Angew. Chem.* **2010**, *122*, 8992–9032; *Angew. Chem. Int. Ed.* **2010**, *49*, 8810–8849; b) M. Melaimi, R. Jazzar, M. Soleilhavoup, G. Bertrand, *Angew. Chem.* **2017**, *129*, 10180–10203; *Angew. Chem. Int. Ed.* **2017**, *56*,10046–10068; c) U. S. D. Paul, U. Radius, *Eur. J. Inorg. Chem.* **2017**, 3362–3375; d) U. S. D. Paul, M. J. Krahfuss, U. Radius, *Chem. Unserer Zeit* **2019**, *53*, 212–223.

[3] a) P. Power, *Nature* **2010**, *463*, 171–177; b) D. Martin, M. Soleilhavoup, G. Bertrand, *Chem. Sci.* **2011**, *2*, 389–399; c) Y. Wang, G. H. Robinson, *Dalton Trans.* **2012**, *41*, 337–345; d) C. D. Martin, M. Soleilhavoup, G. Bertrand, *Chem. Sci.* **2013**, *4*, 3020–3030; e) Y. Wang, G. H. Robinson, *Inorg. Chem.* **2014**, *53*, 11815–11832; f) T. Chu, G. I. Nikonov, *Chem. Rev.* **2018**, *118*, 3608–3680; g) Y. Kim, E. Lee, *Chem. Eur. J.* **2018**, *24*, 19110–19121; h) V. V. Nesterov, D. Reiter, P. Bag, P. Frisch, R. Holzner, A. Porzelt, S. Inoue, *Chem. Rev.* **2018**, *118*, 9678–9842; i) A. Doddi, M. Peters, M. Tamm, *Chem. Rev.* **2019**, *119*, 6994–7112; j) S. Kundu, S. Sinhababu, V. Chandrasekhar, H. W. Roesky, *Chem. Sci.* **2019**, *10*, 4727–4741; k) M. M. D. Roy, A. A. Omaña, A. S. S. Wilson, M. S. Hill, S. Aldridge, E. Rivard, *Chem. Rev.* **2021**, *121*, 12784–12965.

[4] a) Y. Wang, G. H. Robinson, *Dalton Trans.* **2012**, *41*, 337–345; b) D. J. D. Wilson, J. L. Dutton, *Chem. Eur. J.* **2013**, *19*, 13626–13637; c) M. H. Holthausen, J. J. Weigand, *Chem. Soc. Rev.* **2014**,

43, 6639–6657; d) A. Doddi, D. Bockfeld, M. K. Zaretzke, C. Kleeberg, T. Bannenberg, M. Tamm, *Dalton Trans.* **2017**, *46*, 15859–15864; e) L. Dostal, *Coord. Chem. Rev.* **2017**, *353*, 142–158; f) J. E. Borger, A. W. Ehlers, J. C. Slootweg, K. Lammertsma, *Chem. Eur. J.* **2017**, *23*, 11738–11746; g) T. Krachko, J. C. Slootweg, *Eur. J. Inorg. Chem.* **2018**, *24*, 2734–2754; h) K. Schwedtmann, G. Zanoni, J. J. Weigand, *Chem. Asian J.* **2018**, *13*, 1388–1405.

[5] a) O. Back, M. Henry-Ellinger, C. D. Martin, D. Martin, G. Bertrand, *Angew. Chem.* **2013**, *125*, 3011–3015; *Angew. Chem. Int. Ed.* **2013**, *52*, 2939–2943; b) R. R. Rodrigues, C. L. Dorsey, C. A. Arceneaux, T. W. Hudnall, *Chem. Commun.* **2014**, *50*, 162–164; c) S. Roy, K. C. Mondal, S. Kundu, B. Li, C. J. Schurmann, S. Dutta, D. Koley, R. Herbst-Irmer, D. Stalke, H. W. Roesky, *Chem. Eur. J.* **2017**, *23*, 12153–12157; d) Y. Wang, Y. Xie, M. Y. Abraham, R. J. Gilliard, P. Wei, H. F. Schaefer III, P. v. R. Schleyer, G. H. Robinson, *Organometallics* **2010**, *29*, 4778–4780.

[6] a) A. J. Arduengo, J. C. Calabrese, A. H. Cowley, H. V. Dias, J. R. Goerlich, W. J. Marshall, B. Riegel, *Inorg. Chem.* **1997**, *36*, 2151–2158; b) A. J. Arduengo III, H. V. R. Dias, J. C. Calabrese, *Chem. Lett.* **1997**, *26*, 143–144; c) A. K. Adhikari, T. Grell, P. Lönnecke, E. Hey-Hawkins, *Eur. J. Inorg. Chem.* **2016**, *2016*, 620–622; d) N. Hayakawa, K. Sadamori, S. Tsujimoto, M. Hatanaka, T. Wakabayashi, T. Matsuo, *Angew. Chem. Int. Ed.* **2017**, *56*, 5765–5769; *Angew. Chem.* **2017**, *129*, 5859–5863; e) T. Krachko, M. Bispinghoff, A. M. Tondreau, D. Stein, M. Baker, A. W. Ehlers, J. C. Slootweg, H. Grützmacher, *Angew. Chem. Int. Ed.* **2017**, *56*, 7948–7951; *Angew. Chem.* **2017**, *129*, 8056–8059.

[7] a) H. Schneider, D. Schmidt, U. Radius, *Chem. Commun.* **2015**, *51*, 10138–10141; b) M. Bispinghoff, H. Grützmacher, *Chimia* **2016**, *70*, 279–283; c) M. Bispinghoff, A. M. Tondreau, H. Grützmacher, C. A. Faradji, P. G. Pringle, *Dalton Trans.* **2016**, *45*, 5999–6003; d) L. Werner, G. Horrer, M. Philipp, K. Lubitz, M. W. Kuntze-Fechner, U. Radius, *Z. Anorg. Allg. Chem.* **2021**, *647*, 881–895.

[8] a) F. E. Hahn, D. Le Van, M. C. Moyes, T. von Fehren, R. Fröhlich, E. U. Würthwein, *Angew. Chem.* **2001**, *113*, 3241–3244; *Angew. Chem. Int. Ed.* **2001**, *40*, 3144–3148; b) A. Doddi, D. Bockfeld, T. Bannenberg, P. G. Jones, M. Tamm, *Angew. Chem. Int. Ed.* **2014**, *53*, 13568–13572; *Angew. Chem.* **2014**, *126*, 13786–13790; c) M. Cicač-Hudi, J. Bender, S. H. Schlindwein, M. Bispinghoff, M. Nieger, H. Grützmacher, D. Gudat, *Eur. J. Inorg. Chem.* **2016**, *2016*, 649–658; d) D. Heift, Z. Benko, H. Grützmacher, *Dalton Trans.* **2014**, *43*, 5920–5928; e) Z. Li, X. Chen, Y. Li, C.-Y. Su, H. Grützmacher, *Chem. Commun.* **2016**, *52*, 11343–11346.

[9] a) A. Doddi, M. Weinhart, A. Hinz, D. Bockfeld, J. M. Goicoechea, M. Scheer, M. Tamm, *Chem. Commun.* **2017**, *53*, 6069–6072; b) S. Yao, Y. Grossheim, A. Kostenko, E. Ballestero-Martinez, S. Schutte, M. Bispinghoff, H. Grützmacher, M. Driess, *Angew. Chem. Int. Ed.* **2017**, *56*, 7465–7469; *Angew. Chem.* **2017**, *129*, 7573–7577; c) A. Hinz, M. M. Hansmann, G. Bertrand, J. M. Goicoechea, *Chem. Eur. J.* **2018**, *24*, 9514–9519; d) K. M. Melancon, M. B. Gildner, T. W. Hudnall, *Chem. Eur. J.* **2018**, *24*, 9264–9268; e) M. K. Sharma, S. Blomeyer, B. Neumann, H. G. Stammler, A. Hinz, M. van Gastel, R. S. Ghadwal, *Chem. Commun.* **2020**, *56*, 3575–3578; f) A. Schumann, J. Bresien, M. Fischer, C. Hering-Junghans, *Chem. Commun.* **2021**, *57*, 1014–1017; g) J. Krüger, C. Wölper, G. Haberhauer, S. Schulz, *Inorg. Chem.* **2022**, *61*, 597–604.

[10] a) M. Y. Abraham, Y. Wang, Y. Xie, R. J. Gilliard, Jr., P. Wei, B. J. Vaccaro, M. K. Johnson, H. F. Schaefer III, P. v. R. Schleyer, G. H. Robinson, *J. Am. Chem. Soc.* **2013**, *135*, 2486–2488; b) M. Donath, M. Bodensteiner, J. J. Weigand, *Chem. Eur. J.* **2014**, *20*, 17306–17310; c) J. W. Dube, Y. Zheng, W. Thiel, M. Alcarazo, *J. Am. Chem. Soc.* **2016**, *138*, 6869–6877; d) L. P. Ho, A. Nasr, P. G. Jones, A. Altun, F. Neese, G. Bistoni, M. Tamm, *Chem. Eur. J.* **2018**, *24*, 18922–18932; e) A. Doddi, D. Bockfeld, M. K. Zaretzke, T. Bannenberg, M. Tamm, *Chem. Eur. J.* **2019**, *25*, 13119–13123; f) L. P. Ho, M. K. Zaretzke, T. Bannenberg, M. Tamm, *Chem. Commun.* **2019**, *55*, 10709–10712; g) M. Piesch, S. Reichl, M. Seidl, G. Balázs, M. Scheer, *Angew. Chem. Int. Ed.* **2019**, *58*, 16563–16568; *Angew. Chem.* **2019**, *131*, 16716–16721; h) D. Bockfeld, M. Tamm, *Z. Anorg. Allg. Chem.* **2020**, *646*, 866–872.

[11] R. Kretschmer, D. A. Ruiz, C. E. Moore, A. L. Rheingold, G. Bertrand, *Angew. Chem. Int. Ed.* **2014**, *53*, 8176–8179; *Angew. Chem.* **2014**, *126*, 8315–8318.

[12] C. L. Dorsey, R. M. Mushinski, T. W. Hudnall, *Chem. Eur. J.* **2014**, *20*, 8914–8917.

[13] M. M. Siddiqui, S. K. Sarkar, M. Nazish, M. Morganti, C. Kohler, J. Cai, L. Zhao, R. Herbst-Irmer, D. Stalke, G. Frenking, H. W. Roesky, *J. Am. Chem. Soc.* **2021**, *143*, 1301–1306.

[14] L. P. Ho, A. Nasr, P. G. Jones, A. Altun, F. Neese, G. Bistoni, M. Tamm, *Chem. Eur. J.* **2018**, *24*, 18922–18932.

[15] M. S. M. Philipp, M. J. Krahfuss, K. Radacki, U. Radius, *Eur. J. Inorg. Chem.* **2021**, 4007–4019.

[16] A. S. Romanov, M. Bochmann, *Organometallics* **2015**, *34*, 2439–2454.

[17] a) P. B. Hitchcock, C. Jones, J. F. Nixon, *Angew. Chem. Int. Ed.* **1995**, *34*, 492–493; *Angew. Chem.* **1995**, *107*, 522–523; b) C. Jones, J. W. Steed, R. C. Thomas, *J. Chem. Soc. Dalton Trans.* **1999**, 1541–1542; c) C. Jones, *Coord. Chem. Rev.* **2001**, *215*, 151–169; d) P. C. Andrews, J. E. McGrady, P. J. Nichols, *Organometallics* **2004**, *23*, 446–453; e) J. Escudié, H. Ranaivonjatovo, *Organometallics* **2007**, *26*, 1542–1559.

[18] J. B. Waters, Q. Chen, T. A. Everitt, J. M. Goicoechea, *Dalton Trans.* **2017**, *46*, 12053–12066.

[19] a) U. S. D. Paul, U. Radius, *Chem. Eur. J.* **2017**, *23*, 3993–4009; b) H. Schneider, A. Hock, R. Bertermann, U. Radius, *Chem. Eur. J.* **2017**, *23*, 12387–12398; c) H. Schneider, A. Hock, A. D. Jaeger, D. Lentz, U. Radius, *Eur. J. Inorg. Chem.* **2018**, 4031–4043; d) A. Hock, L. Werner, C. Luz, U. Radius, *Dalton Trans.* **2020**, *49*, 11108–11119; e) A. Hock, L. Werner, M. Riethmann, U. Radius, *Eur. J. Inorg. Chem.* **2020**, 4015–4023; f) S. A. Föhrenbacher, V. Zeh, M. J. Krahfuss, N. Ignat'ev, M. Finze, U. Radius, *Eur. J. Inorg. Chem.* **2021**, 1941–1960.

[20] T. Chu, G. I. Nikonov, *Chem. Rev.* **2018**, *118*, 3608–3680.

[21] J. H. J. Berthel, L. Tendera, M. W. Kuntze-Fechner, L. Kuehn, U. Radius, *Eur. J. Inorg. Chem.* **2019**, 3061–3072.

[22] a) M. Ates, H. J. Breunig, A. Soltani-Neshan, M. Tegeler, *Z. Naturforsch. B* **1986**, *41*, 321–326; b) B. A. Chalmers, M. Bühl, K. S. Athukorala Arachchige, A. M. Slawin, P. Kilian, *Chem. Eur. J.* **2015**, *21*, 7520–7531.

[23] V. Lavallo, Y. Canac, C. Prasang, B. Donnadieu, G. Bertrand, *Angew. Chem. Int. Ed.* **2005**, *44*, 5705–5709; *Angew. Chem.* **2005**, *117*, 5851–5855.

[24] G. R. Fulmer, A. J. M. Miller, N. H. Sherden, H. E. Gottlieb, A. Nudelman, B. M. Stoltz, J. E. Bercaw, K. I. Goldberg, *Organometallics* **2010**, *29*, 2176–2179.

[25] G. M. Sheldrick, *Acta Crystallogr. Sect. A* **2014**, *70*, C1437.

[26] a) R. Ahlrichs, M. Bär, M. Häser, H. Horn, C. Kölmel, *Chem. Phys. Lett.* **1989**, *162*, 165–169; b) F. Furche, R. Ahlrichs, C. Hättig, W. Klopper, M. Sierka, F. Weigend, *Wiley Interdiscip. Rev.: Comput. Mol. Sci.* **2014**, *4*, 91–100.

[27] a) M. Häser, R. Ahlrichs, *J. Comput. Chem.* **1989**, *10*, 104–111; b) O. Treutler, R. Ahlrichs, *J. Chem. Phys.* **1995**, *102*, 346–354; c) M. v. Arnim, R. Ahlrichs, *J. Comput. Chem.* **1998**, *19*, 1746–1757; d) F. Weigend, *Phys. Chem. Chem. Phys.* **2002**, *4*, 4285–4291; e) M. Sierka, A. Hogekamp, R. Ahlrichs, *J. Chem. Phys.* **2003**, *118*, 9136–9148.

[28] a) S. Grimme, J. Antony, S. Ehrlich, H. Krieg, *J. Chem. Phys.* **2010**, *132*, 154104; b) S. Grimme, S. Ehrlich, L. Goerigk, *J. Comput. Chem.* **2011**, *32*, 1456–1465.
[29] Y. Zhao, D. G. Truhlar, *Theor. Chem. Acc.* **2007**, *120*, 215–241.
[30] a) A. Schäfer, H. Horn, R. Ahlrichs, *J. Chem. Phys.* **1992**, *97*, 2571–2577; b) A. Schäfer, C. Huber, R. Ahlrichs, *J. Chem. Phys.* **1994**, *100*, 5829–5835; c) K. Eichkorn, O. Treutler, H. Öhm, M. Häser, R. Ahlrichs, *Chem. Phys. Lett.* **1995**, *242*, 652–660; d) K. Eichkorn, F. Weigend, O. Treutler, R. Ahlrichs, *Theor. Chem. Acc.* **1997**, *97*, 119–124; e) F. Weigend, R. Ahlrichs, *Phys. Chem. Chem. Phys.* **2005**, *7*, 3297–3305; f) F. Weigend, *Phys. Chem. Chem. Phys.* **2006**, *8*, 1057–1065.
[31] K. A. Wiberg, *Tetrahedron* **1968**, *24*, 1083–1096.

Manuscript received: February 25, 2022
Revised manuscript received: April 13, 2022
Accepted manuscript online: April 14, 2022

